

## Hydroxyapatite (HA) from Mentarang (Pholas Orientalis) Shells

**Mohd Riza Mohd Roslan, Nashrul Fazli Mohd Nasir, Nur Farahiyah Mohamad, Nur Hafizah**

Biomedical Electronic Engineering Program, Faculty of Engineering Technology  
Electronic,  
University Malaysia Perlis (UniMAP), Perlis, MALAYSIA

\*Corresponding Author Designation

DOI: <https://doi.org/10.30880/mari.2021.02.03.040>

Received 05 September 2021; Accepted 05 October 2021; Available online 15 December 2021

**Abstract** : A huge waste from ocean was created everyday around the world and detrimentally affects the environment. Several species of ocean organisms such as seashells composed high calcium carbonate ( $\text{CaCO}_3$ ) content. In this work, Mentarang (Pholas Orientalis) shells were processed to extract the calcium and progressively synthesized the hydroxyapatite (HA). The as-synthesized HA powder was analyzed via X-Ray Diffraction (XRD) and Fourier Transformed Infrared (FTIR). Evaluation on the pattern and peaks from both analyses resembled the standard HA thus confirm the formation of HA.

**Keywords:** Hydroxyapatite, Mentarang, Pholas Orientalis, Bone Tissue Engineering

### 1. Introduction

Human bone matrix consists of inorganic materials and organic materials at range 60% to 70% and 20% to 30% respectively. Hydroxyapatite (HA) is a group of calcium phosphate composed in bone tissue as an inorganic material [1]. HA with chemical structure  $\text{Ca}_{10}(\text{PO}_4)_6(\text{OH})_2$  widely implemented in bone tissue engineering and other biomedical application due to its biocompatibility properties [2]. Arising of bone tissue engineering implementation indeed due to the rising of clinical bone disease such as bone tumors, infection and bone loss in orthopedic field [3]. Thereby, a lot of researchers work on producing the HA to fulfill this high demand [4]. This consequently drives the synthesizing of HA at economic cost [5] and few researchers came out the idea producing the HA from biogenic resources such as fish scale [6], [7] and seashells [8], [9]. The shells are rich with calcium carbonate ( $\text{CaCO}_3$ ) which can be the source of calcium (Ca) to produce the HA [10]. Synthesizing of HA can be made through several methods such as hydrothermal method [11], [12], sol gel method [13], microemulsion method [14], [15] and chemical precipitation [16], [17]. Generally, chemical precipitation is the most preferable methods as it offers a simple set up, economically and highly yield [18].

This project presents a work synthesizing the HA based on Mentarang (Pholas Orientalis) as its calcium precursor. The usage of seashells waste is a credit to sustain a clean environment against unpleasant odour to surrounding, air and soil pollution and imbalance marine ecosystem [19]. Meanwhile the using of Mentarang (Pholas Orientalis) as the source of calcium precursor is due to its less alkalinity properties compared to the other seashells type hence offered stability when react with phosphoric acid. Chemical precipitation was implemented to process the HA and the final product was characterized by using Fourier Transformed Infrared (FTIR) analysis to study its functional group while X-Ray Diffraction (XRD) in a way investigate its phase and crystallinity.

## 2. Materials and Methods

### 2.1 Materials

Mentarang (Pholas Orientalis) was purchased from local market in Kuala Perlis, Perlis, Malaysia. Phosphoric acid ( $H_3PO_4$ ) with 95% of concentration and ammonia solution ( $NH_3$ ) with 25% of concentration. All the chemicals were used without further purification.

### 2.2 Methods

Chemical precipitation was implemented to synthesis the HA. As the collected Mentarang (Pholas Orientalis) shells were cleaned, the shells waste was grinded to obtain the powder form of calcium carbonate ( $CaCO_3$ ). This  $CaCO_3$  powder was proceed with sintering process to convert to calcium oxide ( $CaO$ ).  $CaO$  is the calcium (Ca) precursor to synthesis the HA while  $H_3PO_4$  is the phosphate precursor. Molarity calcium to phosphate was calculated to 1.67 complying the ratio of HA's Ca/P. As the first step,  $CaO$  was mixed with distilled water and form calcium hydroxide ( $Ca(OH)_2$ ). This followed by  $H_3PO_4$  addition at rate 0.1ml/min. During this process, the overall solution was ensured in pH 11 value and this was done by dropping some  $NH_3$  solution. The product in gelatinous solution was aged for 24hours at room temperature. After 24hours, a white precipitation was formed and filtered by using filter paper. The product is further washed with distilled water and dried in oven at  $110^\circ C$  for 6hours to remove the water completely. The HA cake form was powdered by using mortar. The powder formed is HA and ready for the analysis.

### 2.3 X-Ray Diffraction (XRD) analysis

The phase of HA sample was analysed by XRD analysis using Bruker D2 Phaser. A slight amount of HA powder was compacted into XRD holder and scanned by using the machine. The machine was scanned the powder at scan range  $10^\circ$  to  $90^\circ$  with step size  $0.1^\circ$  and scan rate  $5^\circ/min$ . The raw data were further extracted and analysed by using X'pert Highscore Plus V.2.2.5 software.

### 2.4 Fourier Transformed Infrared (FTIR) analysis

FTIR analysis is mainly to determine the functional group of analysed sample to verify the formation of pure HA. The machine model is FTIR spectrometer Perkin Elmer Spectrum 65 with frequency spectrum of  $400cm^{-1}$  to  $4000cm^{-1}$ .

## 3. Results and Discussion

### 3.1 XRD analysis

The XRD peak of synthesized HA is shows as in Figure 1.  $2\theta$  diffraction peaks values at  $25.85^\circ$ ,  $32.25^\circ$  and  $33^\circ$  are correlate to (002), (112) and (300) Miller's plane of pure HA in PDF 01-074-0565 file. The result shows that the obtained HA is in good agreement with standard data of HA. Basically the peaks presented a high crystallinity of HA and this high crystallinity is characterized by the natural bone [20].

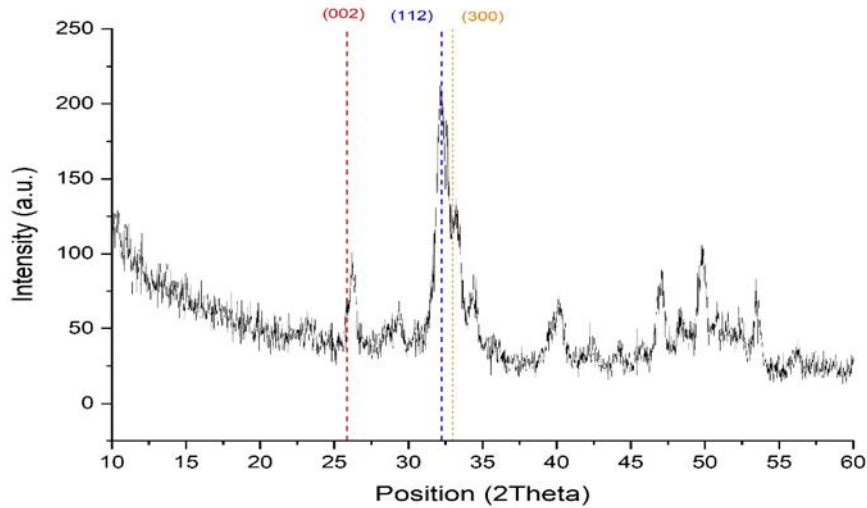


**Figure 1. XRD pattern of synthesized HA**

### 3.2 FTIR analysis

The FTIR wavelength spectrum of synthesized HA is shown as in Figure 2. The spectrum presents two functional groups of HA, which are phosphate ( $\text{PO}_4^{3-}$ ) and hydroxyl (OH), which confirm the formation of HA [21]. The peak at  $1036\text{cm}^{-1}$  indicates the  $\text{PO}_4^{3-}$  peak [22]. On the other hand, OH peaks can be found at  $1640\text{cm}^{-1}$  and  $3300\text{cm}^{-1}$  to  $3600\text{cm}^{-1}$  [23]. This OH peak is implying the hydroxyl group due to the stretching of OH functional group in HA.  $1419\text{cm}^{-1}$  wavenumber corresponds to the carbonate ( $\text{CO}_3^{2-}$ ) peak [24].  $\text{CO}_3^{2-}$  existence was due to the interaction between the free air and distilled water solvent during the synthesizing process [25].

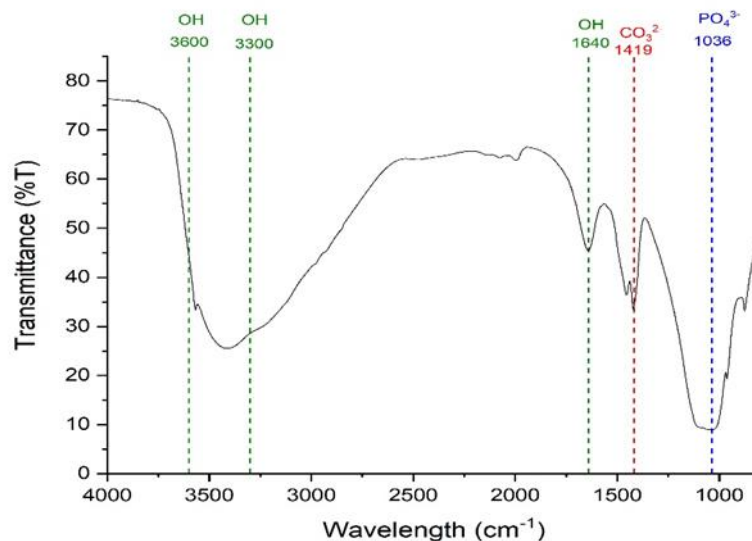


**Figure 2. FTIR pattern of synthesized HA**

## 4. Conclusion

In this project, it can be concluded that HA can be synthesized by using Mentarang (Pholas Orientalis) shells as the calcium precursor. This is affirmed by both characterizations that have been done. The XRD peak of synthesized HA was evaluated and resembles the standard data of HA. Of equal importance, FTIR analysis shows the functional groups of HA, which are  $\text{PO}_4^{3-}$  and OH.

## References

- [1] Z. I. Ahmed, Y. M. Z., El-Sheikh, S. M., & Zaki, "Changes in hydroxyapatite powder properties via heat treatment," *Bull. Mater. Sci.*, vol. 38, no. 7, pp. 1807–1819, 2015.
- [2] L. Li et al., "Surface Modification of Hydroxyapatite Nanocrystallite by a Small Amount of Terbium Provides a Biocompatible Fluorescent Probe," *J. Phys. Chem. C*, vol. 112, no. 32, pp. 12219–12224, Aug. 2008.
- [3] V. Campana et al., "Bone substitutes in orthopaedic surgery: from basic science to clinical practice," *J. Mater. Sci. Mater. Med.*, vol. 25, no. 10, pp. 2445–2461, Oct. 2014.
- [4] M. Z. A. Khiri et al., "Crystallization behavior of low-cost biphasic hydroxyapatite/ $\beta$ -tricalcium phosphate ceramic at high sintering temperatures derived from high potential calcium waste sources," *Results Phys.*, vol. 12, pp. 638–644, Mar. 2019.
- [5] D. Muthu, G. S. Kumar, V. S. Kattimani, V. Viswabaskaran, and E. K. Girija, "Optimization of a lab scale and pilot scale conversion of eggshell biowaste into hydroxyapatite using microwave reactor," *Ceram. Int.*, vol. 46, no. 16, pp. 25024–25034, Nov. 2020.
- [6] S. Paul et al., "Effect of trace elements on the sintering effect of fish scale derived hydroxyapatite and its bioactivity," *Ceram. Int.*, vol. 43, no. 17, pp. 15678–15684, Dec. 2017.
- [7] J. Athinarayanan, V. S. Periasamy, and A. A. Alshatwi, "Simultaneous fabrication of carbon nanodots and hydroxyapatite nanoparticles from fish scale for biomedical applications," *Mater. Sci. Eng. C*, vol. 117, p. 111313, Dec. 2020.
- [8] G. Karunakaran et al., "Sodium dodecyl sulfate mediated microwave synthesis of biocompatible superparamagnetic mesoporous hydroxyapatite nanoparticles using black *Chlamys varia* seashell as a calcium source for biomedical applications," *Ceram. Int.*, vol. 45, no. 12, pp. 15143–15155, Aug. 2019.
- [9] M. R. Roslan et al., "Preliminary study of the polymesoda expansa based hydroxyapatite for medical devices coating application," 2020, p. 020033.
- [10] N. A. S. Mohd Pu'ad et al., "Extraction of Biological Hydroxyapatite from Bovine Bone for Biomedical Applications," *Mater. Sci. Forum*, vol. 1010, pp. 579–583, Sep. 2020.
- [11] K.-W. Jung, S. Y. Lee, J.-W. Choi, and Y. J. Lee, "A facile one-pot hydrothermal synthesis of hydroxyapatite/biochar nanocomposites: Adsorption behavior and mechanisms for the removal of copper(II) from aqueous media," *Chem. Eng. J.*, vol. 369, pp. 529–541, Aug. 2019.
- [12] D. Liu, K. Savino, and M. Z. Yates, "Coating of hydroxyapatite films on metal substrates by seeded hydrothermal deposition," *Surf. Coatings Technol.*, vol. 205, no. 16, pp. 3975–3986, May 2011.
- [13] B. A. E. Ben-Arfa, I. M. M. Salvado, J. M. F. Ferreira, and R. C. Pullar, "Novel route for rapid sol-gel synthesis of hydroxyapatite, avoiding ageing and using fast drying with

- a 50-fold to 200-fold reduction in process time,” *Mater. Sci. Eng. C*, vol. 70, pp. 796–804, 2017.
- [14] F. Foroughi, S. A. Hassanzadeh-Tabrizi, and J. Amighian, “Microemulsion synthesis and magnetic properties of hydroxyapatite-encapsulated nano CoFe<sub>2</sub>O<sub>4</sub>,” *J. Magn. Magn. Mater.*, vol. 382, pp. 182–187, 2015.
- [15] K. Lai, C., Tang, S., Wang, Y., & Wei, “Formation of calcium phosphate nanoparticles in reverse microemulsions,” *Mater. Lett.*, vol. 59, no. 2–3, pp. 210–214, 2005.
- [16] A. F. M. Othman, R., Mustafa, Z., Loon, C. W., & Noor, “Effect of calcium precursors and pH on the precipitation of carbonated hydroxyapatite,” *Procedia Chem.*, no. 19, pp. 539–545, 2016.
- [17] P. Narendran et al., “Influence of pH on wet-synthesis of silver decorated hydroxyapatite nanopowder,” *Colloids Surfaces B Biointerfaces*, vol. 169, pp. 143–150, Sep. 2018.
- [18] A. S. Magdalena Stevanovi, Miodrag J. Luki and M. K. and Z. J. cijevi Nenad Filipovi, “Biomedical inorganic nanoparticles: preparation, properties, and perspectives,” in *Materials for Biomedical Engineering Inorganic Micro and Nanostructures*, 2019, pp. 1–46.
- [19] Saharudin, S. H., Shariffuddin, J. H., Ismail, A., & Mah, J. H. (2018). Recovering value from waste: biomaterials production from marine shell waste. *Bulletin of Materials Science*, 41(6), 162.
- [20] M. Poorraeisi and A. Afshar, “The study of electrodeposition of hydroxyapatite-ZrO<sub>2</sub>-TiO<sub>2</sub> nanocomposite coatings on 316 stainless steel,” *Surf. Coatings Technol.*, vol. 339, pp. 199–207, Apr. 2018.
- [21] D. Walczyk, D. Malina, M. Krol, K. Pluta, and A. Sobczak-Kupiez, “Physicochemical characterization of zinc-substituted calcium phosphates,” *Bull. Mater. Sci.*, vol. 39, no. 2, pp. 525–535, Apr. 2016.
- [22] V. Rodríguez-Lugo et al., “Wet chemical synthesis of nanocrystalline hydroxyapatite flakes: effect of pH and sintering temperature on structural and morphological properties,” *R. Soc. Open Sci.*, vol. 5, no. 8, p. 180962, Aug. 2018.
- [23] A. Pal, P. Nasker, S. Paul, A. Roy Chowdhury, A. Sinha, and M. Das, “Strontium doped hydroxyapatite from *Mercenaria* clam shells: Synthesis, mechanical and bioactivity study,” *J. Mech. Behav. Biomed. Mater.*, vol. 90, pp. 328–336, Feb. 2019.
- [24] J. G. Amaral, J. P. Pessan, J. A. S. Souza, J. C. S. Moraes, and A. C. B. Delbem, “Cyclotriphosphate associated to fluoride increases hydroxyapatite resistance to acid attack,” *J. Biomed. Mater. Res. Part B Appl. Biomater.*, vol. 106, no. 7, pp. 2553–2564, Oct. 2018.
- [25] Y. Sari, M., & Yusuf, “Synthesis and Characterization of Hydroxyapatite based on Green Mussel Shells (*Perna viridis*) with Calcination Temperature Variation Using the Precipitation Method,” *Int. J. Nanoelectron. Mater.*, vol. 11, no. 3, 2018.